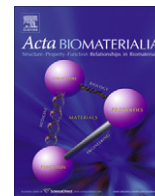




Contents lists available at ScienceDirect

Acta Biomaterialia

journal homepage: [www.elsevier.com/locate/actabiomat](http://www.elsevier.com/locate/actabiomat)

## Poly-L-lysine-coated albumin nanoparticles: Stability, mechanism for increasing *in vitro* enzymatic resilience, and siRNA release characteristics

Harsh Deep Singh<sup>a</sup>, Guilin Wang<sup>a,b</sup>, Hasan Uludağ<sup>a,b,c</sup>, Larry D. Unsworth<sup>a,d,\*</sup>

<sup>a</sup> Department of Chemical and Materials Engineering, Faculty of Engineering, University of Alberta, Edmonton, Alberta, Canada T6G 2G6

<sup>b</sup> Faculty of Pharmacy and Pharmaceutical Sciences, University of Alberta, Edmonton, Alberta, Canada T6G 2G6

<sup>c</sup> Department of Biomedical Engineering, Faculty of Medicine and Dentistry, University of Alberta, Edmonton, Alberta, Canada T6G 2G6

<sup>d</sup> National Research Council, National Institute of Nanotechnology, Edmonton, Alberta T6G 2M9, Canada

### ARTICLE INFO

#### Article history:

Received 19 March 2010  
Received in revised form 10 June 2010  
Accepted 16 June 2010  
Available online xxx

#### Keywords:

BSA  
Coacervation  
PLL  
Coating  
siRNA

### ABSTRACT

Enzymatic degradation of nanoparticle (NP)-based drug delivery vehicles is a major factor influencing the administration routes as well as the site-specific delivery of NPs. To understand the stability of albumin NPs in an aggressive proteolytic environment, bovine serum albumin (BSA) NPs were fabricated via a coacervation technique and stabilized by coating using different molecular weights (MWs: 0.9–24 kDa) and concentrations (0.1–1.0 mg ml<sup>-1</sup>) of the cationic polymer, poly-L-lysine (PLL). A short interfering ribonucleic acid (siRNA) was used as a model drug for encapsulation in the BSA NPs. The generated NPs were characterized for morphology (with atomic force microscopy), size (with photon correlation spectroscopy) and charge (zeta-potential). The size range of formed BSA particles (155 ± 11 to 3800 ± 1600 nm) was effectively controlled by the MW and concentration of the PLL used for coating. The aqueous solution stability of NPs increased with an increasing MW and PLL concentration. However, in the presence of trypsin, NPs coated with higher MW PLL were not as stable as those formed using lower MW PLL. This trend was also confirmed based on the release pattern of siRNA in the presence of trypsin. We conclude that, when designing stabilizing coatings for soft protein-based NPs, smaller molecules may be more suitable for particle coating if enhanced proteolytic resistance and more stable NPs are desired for targeted drug delivery applications.

© 2010 Acta Materialia Inc. Published by Elsevier Ltd. All rights reserved.

### 1. Introduction

Significant efforts have been undertaken in recent years on developing biodegradable nanoparticles (NPs) to deliver a wide range of therapeutic agents, ranging from low-molecular-weight conventional drugs to poly(nucleic acids) [1]. Although several routes for administration of NPs are available (e.g. oral, inhalation and injection), the most convenient drug delivery route is through oral administration and drug uptake *via* the intestine [2,3]. Regardless of the delivery route, however, uncontrolled release of therapeutic agents may result from non-specific degradation of NPs as they traverse through physiological milieu bearing a complex mixture of degrading enzymes. A highly efficient proteolytic enzyme found in all major routes of administration is trypsin [4]. The exposure of NPs to trypsin may lead to premature degradation of NPs, resulting in the loss of therapeutic efficacy. Previous studies have attempted to address this problem for short interfering RNA

(siRNA)-based therapeutic agents by complexing the molecule in NPs composed of 1,2-dioleoyl-3-trimethylammonium-propane and *N*-(polyethylene glycol-2000)-1,2-distearoyl-*sn*-glycero-3-phosphoethanolamine (PEG-DSPE). The PEG moiety in the PEG-DSPE was expected to be located at the periphery (i.e. shell) of the NPs and protect the siRNA against enzymatic degradation and non-specific cellular uptake [5]. As an alternative, NP coating with a suitable material of defined specifications can be employed for preventing or reducing undesirable enzymatic degradation.

The endogenous protein albumin is a suitable material for NP fabrication since it is readily available in large quantities and it metabolizes *in vivo* to produce innocuous degradation products [6]. It can be conveniently fabricated into NPs via coacervation techniques, in which a homogeneous protein solution undergoes phase separation (liquid–liquid) to result in a colloid-rich phase, known as coacervate (containing NPs), and a colloid-poor phase [7]; the size of the NPs can be effectively controlled by the coacervation process parameters [8]. The enzymatic stability of bovine serum albumin (BSA) NPs has been investigated in the presence of proteolytic enzymes [9,10]. Such NPs were shown to be sensitive to trypsin and pepsin, even after being cross-linked with glutaraldehyde. Glutaraldehyde-crosslinked protein NPs made from vicilin

\* Corresponding author. Address: 7th Floor ECERF, Room 7-070 D, 9107 – 116 Street, Edmonton, Alberta, Canada T6G 2V4. Tel.: +1 780 492 6020; fax: +1 780 492 2881.

E-mail address: [larry.unsworth@ualberta.ca](mailto:larry.unsworth@ualberta.ca) (L.D. Unsworth).

were also susceptible to enzymatic degradation; however, increasing crosslinking density with increasing glutaraldehyde treatment resulted in increasing stability against tryptic digestion [11]. To investigate drug release in a proteolytic environment, ganciclovir [9] and 10-hydroxycamptothecin (HCPT) [12] were encapsulated in BSA NPs, and their release was investigated upon being incubated with trypsin. The HCPT release from the NPs was relatively slow but, in the presence of trypsin, the release rate was significantly increased due to degradation of the BSA matrix [11]. The ganciclovir release, however, was only slightly increased in the presence of trypsin. The BSA NPs in the latter case were crosslinked with glutaraldehyde and this process was likely to create a trypsin-insensitive BSA matrix and/or drug coupling to the BSA matrix [9]. However, the use of glutaraldehyde for controlling NP resiliency is a concern since this compound is cytotoxic and it may react undesirably with the therapeutic agents entrapped within the NPs.

Coating the protein NPs with biomaterials may be a superior way to provide protection against enzymatic degradation. Formation of a stable NP through the physical adsorption of a macromolecule will eliminate the need to utilize hazardous crosslinkers in NP formulations. However, no studies probed the effect(s) of coatings on enzymatic degradation of the NPs. Accordingly, the aim of this work was to investigate the degradation of BSA NPs coated with a cationic polymer, poly-L-lysine (PLL). The coatings were created by using different molecular weights (MWs: 0.9–24 kDa) and concentrations (0.1–1.0 mg ml<sup>-1</sup>) of PLL. As trypsin is an inherently robust protease, it was thus employed for enzymatic degradation studies. In addition to directly assessing NP stability, siRNA was encapsulated as a model drug and its release was investigated as an additional measure of NP stability in the presence of trypsin.

## 2. Materials and methods

### 2.1. Materials

BSA and hydrogen bromide salt of PLL of different MWs (0.9, 4.2, 13.8 and 24 kDa) were purchased from Sigma–Aldrich (St. Louis, MO, USA) and used without further purification. FAM-labelled siRNA (double stranded, 21 base pairs) was purchased from Ambion Inc. (Austin, TX, USA). EDTA–trypsin, 10× (Invitrogen, Carlsbad, CA, USA), was diluted 1:10 with 1× Hank's buffered salt solution to 1× (0.05 g l<sup>-1</sup>) concentration before use. Fluorescence isothiocyanate (FITC; Pierce, Rockford, IL, USA) was used to label the PLL and BSA. Sodium phosphate, monobasic, monohydrate sodium phosphate and sodium chloride laboratory-grade reagents were purchased from EMD Chemical Inc. (Darmstadt, Germany). Ethanol was purchased from Fischer Scientific (Ottawa, Ontario, Canada).

### 2.2. Preparation of albumin nanoparticles

BSA NPs were prepared via a coacervation technique as detailed elsewhere [8,13]. Briefly, 250 µl of an aqueous BSA (10 mg ml<sup>-1</sup>) solution was added to an equal volume of 10 mM aqueous NaCl solution in glass vials (Kimble Glass Incorporation, Vineland, NJ, USA), and stirred (15 min at 600 rpm, room temperature). Fresh flasks were used for making NPs each time. When siRNA encapsulation was desired, siRNA solution (10 µl of 0.15 mg ml<sup>-1</sup>) was stirred (600 rpm for 1 h at room temp) with this BSA solution. NPs were formed by adding ethanol (final volume ratio of ethanol to starting BSA solution = 6) dropwise to the BSA solution while being stirred (600 rpm). Stirring was continued for 3 h after the complete addition of ethanol. To stabilize the NPs, PLL of MWs 0.9, 4.2, 13.8 and 24 kDa at various concentrations (0.1, 0.3 and 1.0 mg ml<sup>-1</sup>) in deionized water were introduced to the system; 500 µl of these PLL

solutions was added dropwise to the equal volume of BSA NPs suspension, under constant shaking of 500 rpm (Labnet, Woodbridge, NJ, USA). Shaking was continued for 1 h at room temperature.

### 2.3. FITC labeling of PLL (FITC–PLL) and BSA

The FITC-labeled PLL was used to determine the overall coating efficiency and its effect on stabilizing BSA NPs. The FITC–PLL was obtained by incubating 10 µl of 0.1 mM FITC solution (in DMSO) with 1 ml of PLL (2 mg ml<sup>-1</sup> in 100 mM phosphate buffer, pH 7.4) for 1 h at room temperature. Ethanol (9 ml) was then added to this solution and the solution was centrifuged at 3000 rpm for 15 min at room temperature, and the supernatant was removed. The pellet formed during this process was washed with 5 ml of ethanol and centrifuged for 15 min, at 3000 rpm. The solids obtained were dried under vacuum for 5 h and stored in the dark at 4 °C until used. BSA labeling was conducted using similar procedures, except the BSA concentration was 10 mg ml<sup>-1</sup>.

### 2.4. FITC–PLL coating of BSA NPs

FITC–PLL coating efficiency was determined using fluorescence measurements, where NPs were formed using previously defined FITC–PLL MWs and solution concentrations. Equal volumes of phosphate buffer (300 µl, pH 7.4) and coated NPs suspension were centrifuged (15,000 rpm, 1 h) and the fluorescence ( $\lambda_{\text{ex}}$ : 485 nm;  $\lambda_{\text{em}}$ : 527 nm) of the supernatant was analyzed using a multiwell plate reader (Thermo Labsystems, Franklin, MA, USA). Using a calibration curve, the coating efficiency was calculated as:  $(1 - (\text{FITC} - \text{PLL}_{\text{supernatant}} / \text{FITC} - \text{PLL}_{\text{initial}})) \times 100\%$ .

### 2.5. NP characterization

Coated and uncoated BSA NPs were analyzed using atomic force microscopy (AFM; MFP-3D, Asylum Research, Santa Barbara, CA, USA), photon correlation spectroscopy (PCS) and zeta-potential ( $\zeta$ -potential) assessment. AFM analysis utilized an AC 240TS cantilever throughout measurements to determine particle size and the presence of aggregate formation. AFM samples were prepared by adding 45 µl of phosphate buffer (10 mM, pH 7.4) to 5 µl of NP sample, sonicating for 3 min to reduce aggregate formation and air drying (room temperature) the sample onto PELCO<sup>R</sup> Mica discs (TED PELLA, Inc.; Redding, CA, USA). Igor Pro imaging software (version 5.04 B) was used to analyze generated images. The mean particle size of the coated and uncoated BSA NPs were determined by dynamic light scattering (Zetasizer 3000 HS, Malvern Instruments Ltd., UK) using a 633 nm He–Ne laser at a scattering angle of 90°. Uncoated BSA NPs were used directly for the measurements and PLL-coated BSA NPs were diluted 1:2 with phosphate buffer (10 mM, pH 7.4). The surface charge of these NPs was determined by measuring their electrophoretic mobility using the same instrument at 25 °C.

### 2.6. Stability of BSA NPs

The NPs were formed using the procedure discussed previously, except BSA solutions included 5% of FITC–BSA as a tracer. The PLL-stabilized BSA NPs were diluted by equal volumes of phosphate buffer (10 mM, pH 7.4, 0.02% sodium azide) for all stability tests with or without trypsin addition. NP suspensions were incubated with and without trypsin (room temperature), using a BSA:trypsin ratio of 250 (w:w), on an orbital shaker (Labnet shaker, Orbit P4) at 500 rpm. The FITC–BSA released to the supernatant was collected as discussed previously. At 0, 1, 3 and 7 days, 500 µl of the sample was recovered and centrifuged at 15,000 rpm for 1 h. Supernatant fluorescence ( $\lambda_{\text{ex}}$ : 485 nm;  $\lambda_{\text{em}}$ : 527 nm) was determined, using a

calibration curve, and the release of FITC–BSA was calculated as  $(1 - (\text{FITC} - \text{BSA}_{\text{supernatant}}/\text{FITC} - \text{BSA}_{\text{initial}})) \times 100\%$ .

### 2.7. Tryptic degradation of siRNA-loaded coated and uncoated BSA NPs

FAM-labeled siRNA was used to study the release kinetics of siRNA from various PLL-coated BSA NPs, in the absence and presence of trypsin. In all cases, a PLL concentration of  $1.0 \text{ mg ml}^{-1}$  was used for coating the NPs and release values were normalized to 0% for day 0. The resultant PLL-coated NP suspensions were dialyzed (MW cutoff 25 kDa) against 1 mM NaCl ( $3 \times$ , 16 h between replacement), then diluted with equal volumes of phosphate buffer (10 mM, pH 7.4, 0.02% sodium azide). On the orbital shaker (500 rpm), these suspensions were incubated (room temp) with and without trypsin, the BSA to enzyme ratio being kept at 250 (w:w). The amount of siRNA in the supernatant was determined using a calibration curve and the release was calculated as  $(1 - (\text{FAM} - \text{siRNA}_{\text{supernatant}}/\text{FAM} - \text{siRNA}_{\text{encapsulated}})) \times 100\%$ .

## 3. Results and discussion

### 3.1. PLL adsorption onto BSA NPs and the $\zeta$ -potential

Given that the  $pK_a$  of the  $\epsilon\text{-NH}_2$  group in PLL is  $\sim 10.5$ , the PLL is expected to be positively charged under the experimental pH conditions in this study [4]. Thus, anionic BSA should interact electrostatically with the cationic PLL, leading to its adsorption onto the NPs. The amount of PLL adsorption on NPs was examined as a function of PLL MW and concentration. As shown in Fig. 1A, the amount of adsorbed 0.9, 4.2 and 24 kDa PLL increased with PLL concentration. Adsorbed amounts for 0.9 and 4.2 kDa PLL were similar, and increased from  $\sim 50$  to  $250 \mu\text{g}$  of PLL per mg of BSA for 0.1 and  $1 \text{ mg ml}^{-1}$  PLL, respectively. These polymers did not show a plateau in adsorption, possibly indicating that the surface was not saturated with PLL. The adsorbed amount of 24 kDa PLL increased from  $\sim 55$  to  $140 \mu\text{g}$  of PLL per mg BSA for PLL concentrations of 0.1 and  $1.0 \text{ mg ml}^{-1}$ , respectively. Unlike the 0.9 and 4.2 kDa PLLs, 24 kDa PLL adsorption approached a plateau value, suggesting that the surface area of the NP solution was saturated at  $\sim 140 \mu\text{g}$  of PLL per mg of BSA for this polymer. The likely reason for higher adsorbed amounts of 0.9 and 4.2 kDa PLL could be that the surface area accessible for lower MW PLLs is larger as compared to the higher MW PLL. It is also possible that the smaller PLLs may penetrate into the NP surfaces, leading to the observed increase in adsorption.

Uncoated and coated BSA NPs were characterized for their  $\zeta$ -potential (Fig. 1B); the  $\zeta$ -potential of uncoated BSA NPs was  $-11 \text{ mV}$ , which is in agreement with the previously reported  $\zeta$ -potential of  $-10 \text{ mV}$  for BSA NPs formed using ethanol as the desolvation agent [14]. The  $\zeta$ -potential of BSA NPs increased upon PLL coating, where a  $\zeta$ -potential as high as  $20.6 \pm 0.4 \text{ mV}$  was observed. The  $\zeta$ -potentials of NPs formed using 0.1, 0.3 and  $1.0 \text{ mg ml}^{-1}$  of 0.9 kDa PLL were  $3.1 \pm 0.2$ ,  $6.7 \pm 2.1$  and  $10.1 \pm 1.7 \text{ mV}$ , respectively. The  $\zeta$ -potentials of NPs formed using 4.2 kDa PLL were  $10.8 \pm 2.6$ ,  $9.1 \pm 1.9$  and  $12.3 \pm 0.26 \text{ mV}$  for PLL concentration of 0.1, 0.3 and  $1 \text{ mg ml}^{-1}$ , respectively. The increase in NP  $\zeta$ -potential with increasing concentration of 0.9 and 4.2 kDa PLL supports the results presented in Fig. 1A. The  $\zeta$ -potential for NPs formed using 24 kDa PLL were  $19.3 \pm 0.3$ ,  $19.4 \pm 0.6$  and  $20.4 \pm 0.2 \text{ mV}$ , respectively. This trend was in agreement with the adsorption plateau observed for the 24 kDa PLL (Fig. 1A). Unlike the current study, which indicated no difference in  $\zeta$ -potential with the concentration of 24 kDa PLL, such an effect was observed when the concentration was varied between 0.01 and  $0.1 \text{ mg ml}^{-1}$  in an earlier work [8], perhaps indicating that saturation levels of 24 kDa PLL are easily

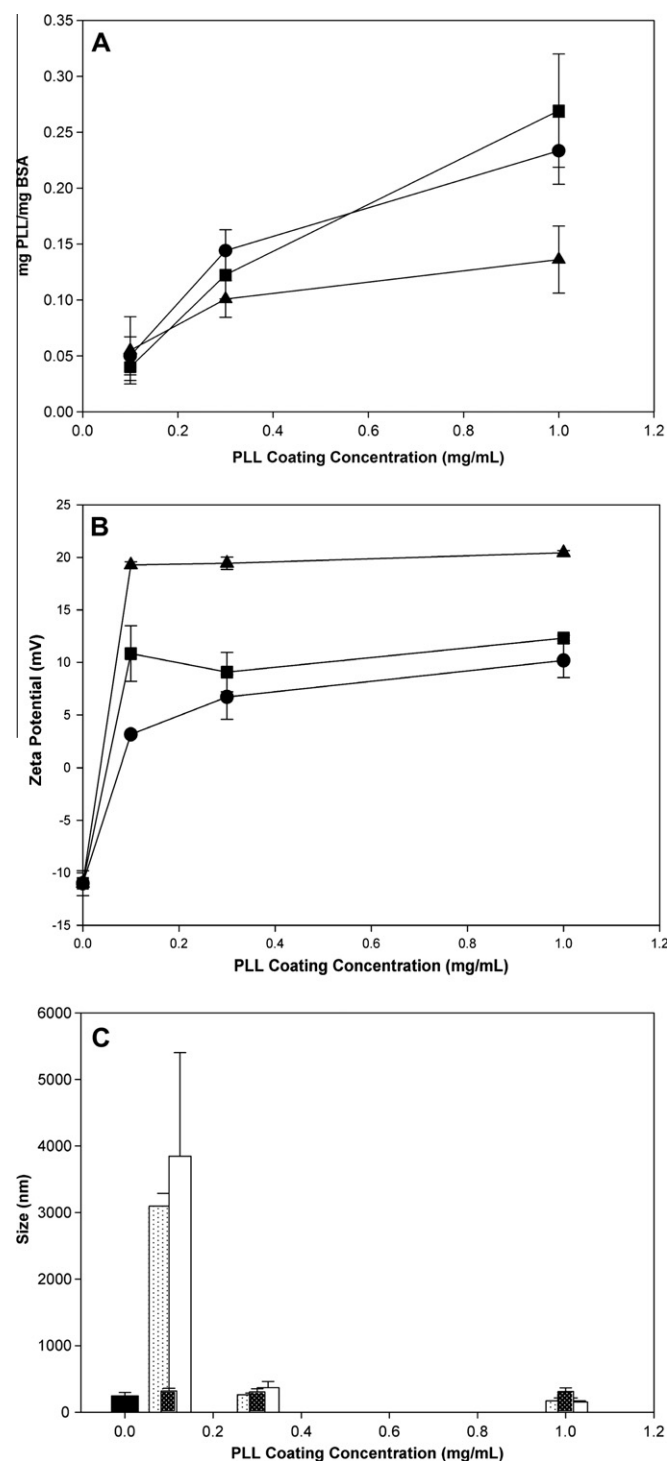


**Fig. 1.** The amount of PLL adsorbed onto BSA NPs (A), zeta-potential of NPs (B), and average particle diameter of the particles (C). PLL MWs used were 0.9 (●), 4.2 (■, □) and 24 (▲, ▨) kDa. The amount of FITC–PLL adsorbed onto BSA NPs increased with the increasing concentration of 0.9 and 4.2 kDa PLL. A plateau was observed for the adsorbed amount of 24 kDa PLL onto BSA NPs. The zeta-potential of BSA NPs increased significantly upon coating. Twenty-four kilodaltons PLL-coated BSA NPs gave the highest zeta-potentials of  $\sim 20 \text{ mV}$  with almost no change with increasing concentration of PLL. A large increase in the particle size was noted for BSA NPs coated with  $0.1 \text{ mg ml}^{-1}$  of 0.9 and 4.2 kDa PLL.

reached for this system. The differences in the  $\zeta$ -potentials of BSA NPs coated with 24 and 4.2 kDa and with 24 and 0.9 kDa PLL were found to be statistically different ( $p < 0.05$ , single-factor analysis of

variance (ANOVA)), contrary to BSA NPs coated with 0.9 and 4.2 kDa PLL, where the difference was not statistically different ( $p > 0.05$ , single-factor ANOVA).

### 3.2. Effect of PLL coating conditions on NP size

Based on the PCS analysis (Fig. 1C), the mean particle diameter of uncoated BSA NPs was observed to be  $247 \pm 50$  nm, which was similar to the previously reported value of  $260 \pm 20$  nm for NPs prepared in a similar manner [8]. A drastic increase in the diameter of NPs formed using a PLL solution concentration of  $0.1 \text{ mg ml}^{-1}$  was observed to be  $3.1 \pm 0.2$  and  $3.8 \pm 1.6 \mu\text{m}$  for 0.9 and 4.2 kDa PLL, respectively. However, for PLL MWs of 0.9 and 4.2 kDa in solution concentrations of 0.3 and  $1 \text{ mg ml}^{-1}$ , significantly smaller NP diameters were observed. NPs formed using solution concentrations of 0.3 and  $1.0 \text{ mg ml}^{-1}$  of 0.9 kDa PLL were determined to be  $265 \pm 22$  and  $170 \pm 47$  nm, and for 4.2 kDa PLL diameters were  $370 \pm 92$  and  $155 \pm 11$  nm, respectively. Patch flocculation mechanisms may explain this observed NP increase; patchy adsorption of the cationic PLL onto the negatively charged BSA surface led to enhanced electrostatic interactions that drove the system to aggregation [15]. The same phenomenon was observed in an earlier work for NPs developed from PEGylated poly(lactic acid) and poly(lactic-co-glycolide) acid [16]; NPs developed from these copolymers having low PEG content showed aggregation possibly because of incomplete coverage of the surfaces of NPs by PEG chains.

NP diameters of  $321 \pm 40$ ,  $306 \pm 47$  and  $313 \pm 54$  nm were observed for NPs coated with 24 kDa PLL at concentrations of 0.1, 0.3 and  $1.0 \text{ mg ml}^{-1}$ , respectively. No large particle size for BSA NPs coated with  $0.1 \text{ mg ml}^{-1}$  of 24 kDa PLL was observed. Consistent with adsorption amounts, it is clear that the 24 kDa PLL is able to saturate the surface of BSA NPs, which probably results in the “full” surface coverage that prevents the large-scale aggregation of BSA NPs.

BSA NPs were analyzed with AFM (Fig. 2) to confirm the size of the particles measured by the PCS. Despite the appearance of some aggregates, uncoated BSA NPs appeared to be spherical particles that were  $\sim 150$  nm in diameter. These values appeared to be smaller than the ones recorded from PCS, probably because of shrinkage

of the particles during the drying process necessary for AFM imaging. Coating the BSA NPs with  $0.3 \text{ mg ml}^{-1}$  of 0.9, 4.2 and 24 kDa PLL resulted in average particle diameters of  $\sim 200$ ,  $\sim 180$  and  $\sim 250$  nm under AFM, respectively. It appeared that the particle size and shape were less uniform for NPs formed with 0.9 and 4.2 kDa PLL. Compared to PCS measurements, these particles were again smaller in size (typically in the 100–250 nm range), probably due to shrinkage of particles during the drying process. However, the BSA NPs coated with  $0.3 \text{ mg ml}^{-1}$  of 24 kDa PLL had a more uniform size distribution and were more spherical.

### 3.3. NP stability with trypsin

The stability of the BSA NPs was evaluated by quantitating the release of BSA from the NPs as a function of time. As unmodified BSA NPs were extremely fragile and unstable in solution (i.e. visible aggregates were seen upon prolonged incubation), BSA release only from the PLL-coated NPs were investigated.

The release of BSA from PLL-coated BSA NPs in the absence of trypsin was studied (Fig. 3). BSA release from 0.9 kDa PLL-coated NPs was found to be highest, where the cumulative BSA release after 7 days was observed to be  $35 \pm 3$ ,  $29 \pm 5$  and  $20 \pm 4\%$  for BSA NPs formed using 0.1, 0.3 and  $1 \text{ mg ml}^{-1}$  of PLL concentration. The relatively high release of BSA from the NPs coated with 0.9 kDa was indicative of an unstable coating, which was unable to retain the BSA within the NP matrix. The decrease in the cumulative BSA release with increasing PLL concentration was also consistent with the need for a better PLL coating for a stable BSA matrix. The cumulative release of BSA from 4.2 kDa PLL-coated NPs was  $22 \pm 7$ ,  $19 \pm 4$  and  $18 \pm 3\%$  for coating concentrations of 0.1, 0.3 and  $1.0 \text{ mg ml}^{-1}$ , respectively. BSA NPs coated with 0.1, 0.3 and  $1 \text{ mg ml}^{-1}$  concentrations of 13.8 and 24 kDa PLL showed cumulative releases of  $26 \pm 2$ ,  $19 \pm 5$  and  $17 \pm 2\%$  and  $21 \pm 3$ ,  $18 \pm 5$  and  $16 \pm 3\%$ , respectively, after 7 days of incubation. Cumulative BSA release decreased with increasing concentration of PLL for these PLLs as well. However, it was apparent that increasing the PLL MW to greater than 4.2 kDa did not seem to have a large effect on the BSA release from the NPs.

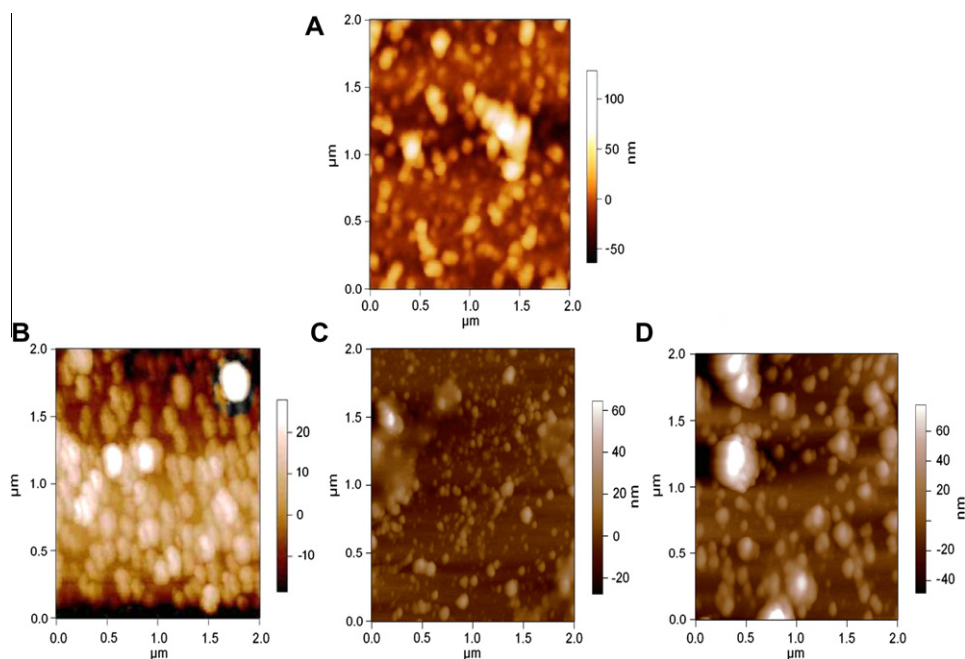


**Fig. 2.** Representative AFM pictures (height image mode) of uncoated and uncoated BSA NPs. Uncoated BSA NPs (A), BSA NPs coated with  $0.3 \text{ mg ml}^{-1}$  of 0.9 (B), 4.2 (C) and 24 (D) kDa PLL. Larger NPs were observed with coating. Uniform and spherical NPs were observed with increasing MW of PLL.



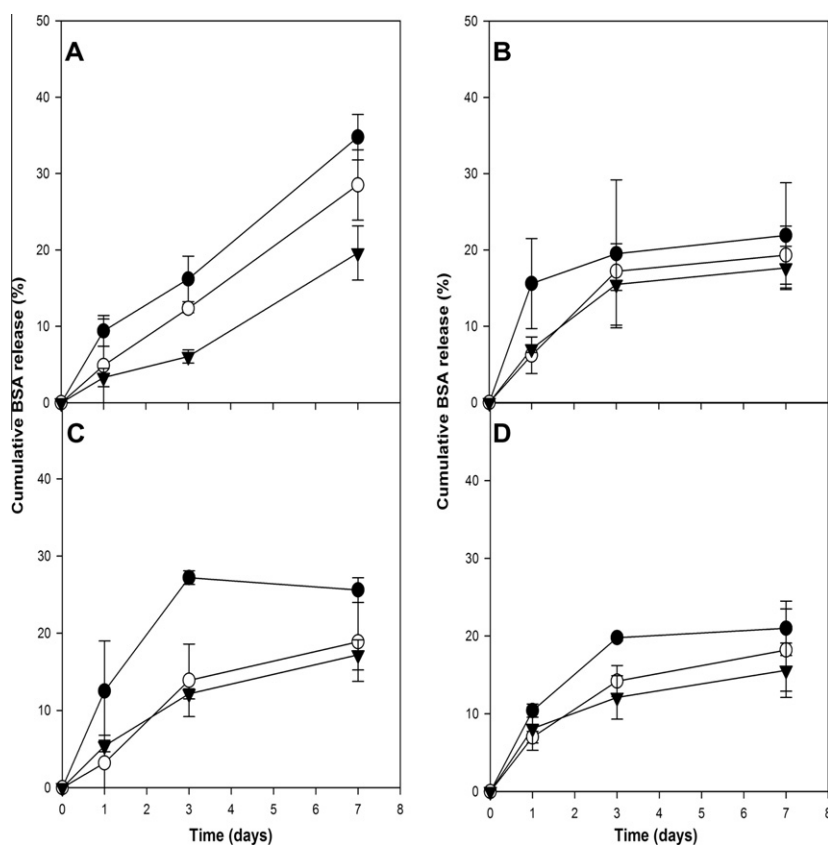


**Fig. 3.** Stability of PLL-coated BSA NPs based on release profile of FITC-BSA from coated BSA NPs. BSA NPs formed via coacervation were coated with PLL and release of FITC-BSA was measured in phosphate buffer (pH 7.4). The MWs of PLL used for coating onto BSA NPs were 0.9 (A), 4.2 (B), 13.8 (C) and 24 (D) kDa, with their concentrations being 0.1 (●), 0.3 (○) and 1.0 (▼) mg ml<sup>-1</sup>, respectively. Trend lines are provided as a guide to the eye. Data points represent an average of  $n \geq 3$ ; error bars are  $\pm 1$  SD. Continuous release of FITC-BSA from 0.9 kDa PLL-coated BSA NPs and almost no release of FITC-BSA from 4.2, 13.8 and 24 kDa PLL-coated BSA NPs after day 3 were observed.

The stability of BSA NPs coated with 0.3 mg ml<sup>-1</sup> of 0.9 and 24 kDa PLL (Fig. 4) was also studied using AFM. The 0.9 kDa PLL-coated NPs increased in size from  $\sim 200$  nm to  $>500$  nm over the study period of 7 days. An increase in the NP aggregation was also observed with time. In contrast, NPs coated with 24 kDa PLL under similar conditions showed a minimal increase in particle size from  $\sim 200$  to  $\sim 300$  nm over the 7 day study period. The low  $\zeta$ -potential (6.7 mV) of the BSA NPs coated with 0.3 mg ml<sup>-1</sup> of 0.9 kDa PLL was not large enough to prevent aggregation, whereas the BSA NPs coated with 0.3 mg ml<sup>-1</sup> of 24 kDa PLL had a large  $\zeta$ -potential (19.5 mV) that may have significantly inhibited NP aggregation.

BSA release in the presence of trypsin (Fig. 5) was higher for all NPs compared to BSA release in the absence of trypsin. Direct control data for trypsin-induced release was comparable to the results shown in Fig. 3, as expected. Minor deviations are likely due to the batch-to-batch variations in NP formation. Thus A1, B1 and C1 in Fig. 5 were incorporated to fully understand the effect of trypsin directly upon NP digestion. Upon exposure to trypsin, NPs formed with 0.1, 0.3 and 1.0 mg ml<sup>-1</sup> 0.9 kDa PLL released  $59 \pm 3$ ,  $44 \pm 2$  and  $30 \pm 3\%$  of encapsulated BSA after 7 days, respectively. In the absence of trypsin, the corresponding values were  $32 \pm 1$ ,  $27 \pm 6$  and  $23 \pm 2\%$ , respectively. For BSA NPs coated with 4.2 kDa PLL, the BSA release was  $23 \pm 1$ ,  $17 \pm 6$  and  $17 \pm 5\%$  for coating concentrations of 0.1, 0.3 and 1.0 mg ml<sup>-1</sup>, respectively, in the absence of trypsin. Upon exposure to trypsin, these NPs released  $57 \pm 2$ ,  $50 \pm 3$  and  $18 \pm 1\%$  of encapsulated BSA. The BSA release from NPs coated with 0.1, 0.3 and 1.0 mg ml<sup>-1</sup> of 24 kDa PLL was  $19 \pm 1$ ,  $19 \pm 2$  and  $22 \pm 0\%$  in the absence of trypsin. The corresponding values in the presence of trypsin were noted to be  $61 \pm 2$ ,  $54 \pm 1$  and  $48 \pm 6\%$ , respectively. Increases in BSA release were almost double for some

systems upon exposure to trypsin. The differences in the cumulative BSA release in the presence and absence of trypsin were found to be statistically significant for all the coating concentrations on day 1 ( $p < 0.05$ , ANOVA: single factor). An exception to this was observed for 0.9 and 4.2 kDa PLL for coating concentration of 1 mg ml<sup>-1</sup>, where the BSA release was unaffected with trypsin.

An interesting observation is the decrease, over time, in the cumulative release of BSA with the increasing concentration of PLL (0.9 and 4.2 kDa) used for coating BSA NPs. As shown in Fig. 1A, there was no saturation noted for the adsorbed amount of the lower MW PLLs onto the BSA NPs, but the onset of a plateau may be evident for the 24 kDa PLL system; as a result, there is an intimate surface coverage of the NPs at higher concentrations. Therefore, at a coating concentration of 0.1 mg ml<sup>-1</sup> (for both 0.9 and 4.2 kDa PLL), a slight cleavage by trypsin resulted in quick disintegration of the NPs and, hence, the large release of BSA. However, the NPs coated with 24 kDa PLL seemed to be overly sensitive to the trypsin treatment (unlike lower MW PLLs). This could be due to the tendency of high MW PLL to display more loops, tails and trains while in the adsorbed state [15], thereby being more accessible to trypsin hydrolysis. The saturation noted for the 24 kDa PLL adsorption (Fig. 1A) could also explain the similar BSA release rates (i.e. degradation rate) observed at the three coating concentrations.

### 3.4. siRNA encapsulation in BSA NPs

siRNA has attracted much attention as a therapeutic agent and may be used to treat lethal diseases requiring systematic administration to enter target cells [17]. However, siRNA degrades rapidly

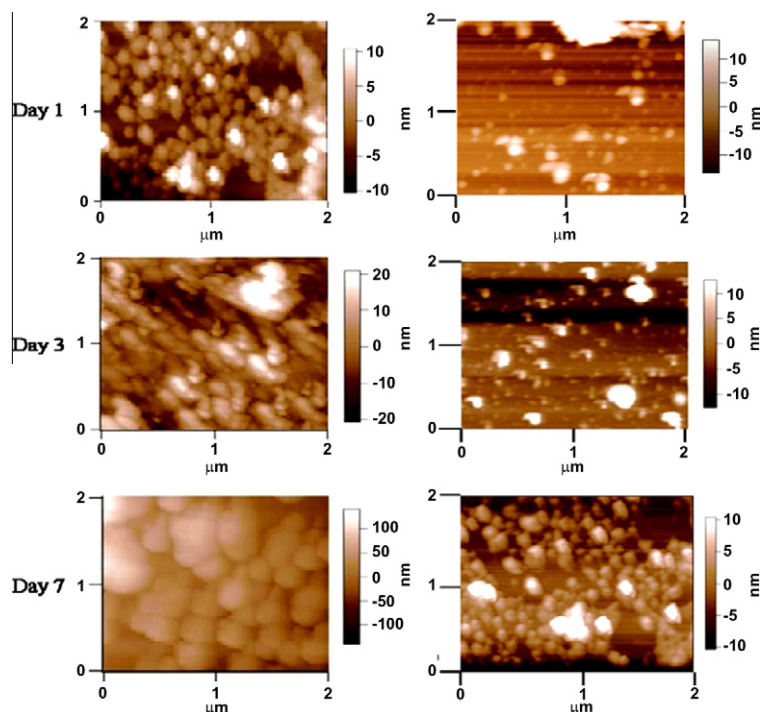


**Fig. 4.** AFM pictures of coated BSA NPs. BSA NPs coated with  $0.3 \text{ mg ml}^{-1}$  of 0.9 (left column) and 24 (right column) kDa PLL. PLL-coated BSA NPs suspensions were diluted with phosphate buffer (pH 7.4) and incubated. Samples were analyzed under AFM at Day 1, 3 and 7. An increase in the particle size as well as aggregation was observed for 0.9 kDa PLL-coated BSA NPs. Partial increase in the particle size was noted with time for 24 kDa PLL-coated BSA NPs.

in the circulation and cellular cytoplasm, resulting in a short half-life [18]. A carrier system is therefore needed where siRNA is not in direct contact with the physiological environment. For example, siRNA encapsulated in hydrogel NPs resulted in improved stability and better receptor breakdown [19]. Herein, siRNA was encapsulated in BSA NPs, where the encapsulation efficiency was assessed using a FAM-labeled siRNA. The encapsulation efficiency was found to increase from  $12 \pm 3\%$  for uncoated BSA NPs to  $>50\%$  for coated BSA NPs. Also, an increase in the encapsulation efficiency was observed with increasing PLL MW. Encapsulation efficiencies of  $58 \pm 5\%$ ,  $66 \pm 6\%$  and  $83 \pm 6\%$  were observed for BSA NPs coated with  $1.0 \text{ mg ml}^{-1}$  of 0.9, 4.2 and 24 kDa PLL, respectively. It is thought that the low encapsulation efficiency of siRNA in uncoated NPs was largely due to the inherent instability of the uncoated NP. Moreover, because the siRNA is added to the BSA solution and the particles are coacervated prior to the PLL addition, it stands to reason that the siRNA would be largely incorporated within the NPs. This charged layer may be able to hinder the molecular mobility of siRNA and inhibit it from leaving the BSA matrix during the fabrication process. An analogous observation was reported when cationic polyethylenimine (PEI) was used to coat poly(D,L-lactide-co-glycolide) NPs: the encapsulation efficiency of siRNA was increased from 43% to 80% upon PEI coating [20]. The increase in the number of positive moieties with increasing PLL MW might be the reason for the increase in the encapsulation efficiency with the use of higher MW PLL.

### 3.5. siRNA release from uncoated and coated NPs in the presence of trypsin

The release profile of siRNA encapsulated in NPs was investigated in the absence and presence of trypsin (Fig. 6). The net release of siRNA from BSA NPs coated with  $1.0 \text{ mg ml}^{-1}$  of 0.9, 4.2 and 24 kDa PLL released  $2.4 \pm 0.45$ ,  $3.44 \pm 0.3$  and  $5.2 \pm 0.4 \text{ ng}$  of encapsulated siRNA, respectively, in the presence of trypsin after

7 days of study period. In the absence of trypsin, the corresponding values were  $1.8 \pm 0.4$ ,  $1.3 \pm 0.1$  and  $1.35 \pm 0.32 \text{ ng}$ , respectively. The release was higher in the presence of trypsin, and the higher MW PLLs (4.2 and 24 kDa) gave a higher release rate upon trypsin digestion as compared to the 0.9 kDa PLL coating. The increase in the amount of siRNA released from the coated NPs was in line with the increased BSA release noted with increased PLL MW in the presence of trypsin. On exposure to trypsin, the more accessible domains of the larger 24 kDa PLL resulted in easier degradation, facilitating a larger release of siRNA compared to other lower MW PLLs.

Increasing drug (siRNA in our case) release upon trypsin treatment is expected from proteolytically sensitive protein NPs. BSA NPs containing HCPT, for example, displayed such an enhanced release upon trypsin exposure:  $\sim 25\%$  release in 40 h in the absence of trypsin but  $\sim 90\%$  release in 20 h in the presence of trypsin [12]. The release of some molecules (e.g. Rose Bengal as a model drug) from human serum albumin (HSA) NPs was relatively slow – perhaps too slow for practical application. However, the presence of trypsin accelerated the release rate of the encapsulated drug from these NPs, making them more practical for drug release [21]. Compared to native HSA NPs, preparing HSA NPs with PEG moieties on the surface appeared to reduce the trypsin-stimulated release [20], indicating an inhibitory effect of the PEG layer on protein degradation by the trypsin. In this regard, PEG might act in a similar way to PLL coatings used in this study, impeding the access of trypsin to the NP core. It might be possible to incorporate PEG along with cationic polymers for particle coatings in order to fine-tune the proteolytic sensitivity of protein NPs.

## 4. Conclusions

This study described a method of obtaining BSA NPs in a practical range. There was a large increase in the zeta-potential of the BSA NPs upon PLL coatings, where the BSA NPs coated with

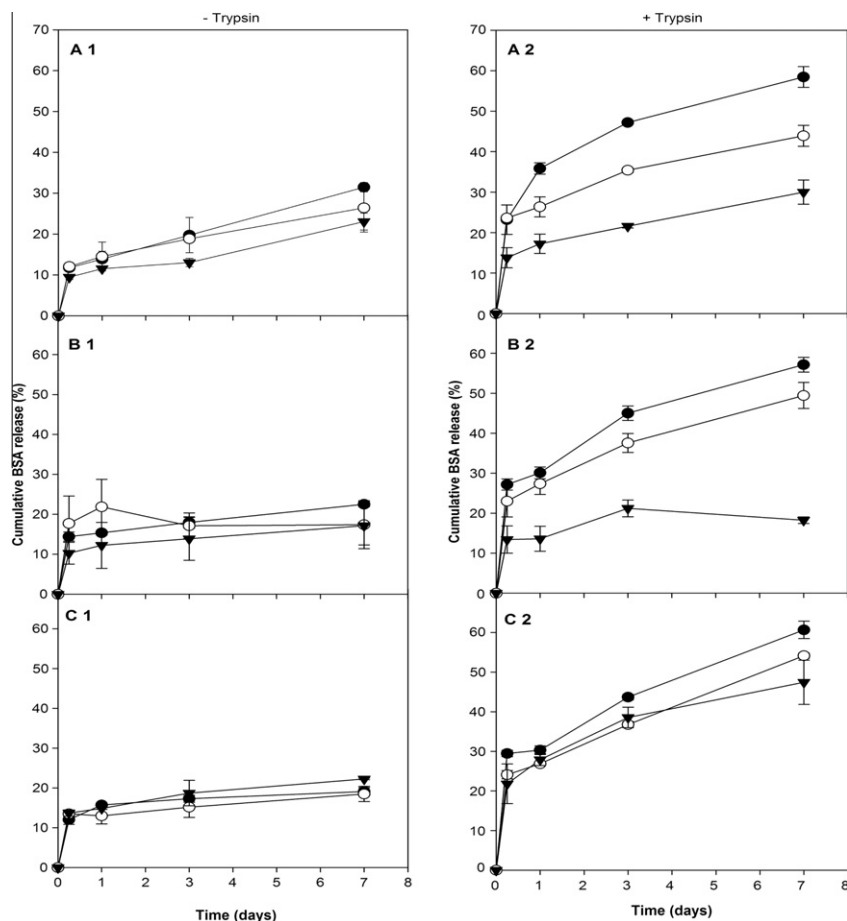


**Fig. 5.** Tryptic digestion of PLL-coated FITC-BSA NPs based upon a fluorescence test. Fluorescence value of the supernatant was calculated in the absence and presence of trypsin. PLL MWs were varied from 0.9 (A1, A2) to 4.2 (B1, B2) and 24 (C1, C2) kDa. Symbols (●), (○) and (▼) represent FITC-BSA release from 0.1, 0.3 and 1.0 mg ml<sup>-1</sup>, respectively, of PLL-coated BSA NPs. Trend lines are provided as a guide to the eye. Data points represent an average of  $n \geq 3$ ; error bars are  $\pm 1$  SD. Trypsin was found to digest the coated BSA NPs. The digestion rate was found to decrease with increasing concentration of the 0.9 and 4.2 kDa PLL used for coating onto BSA NPs.

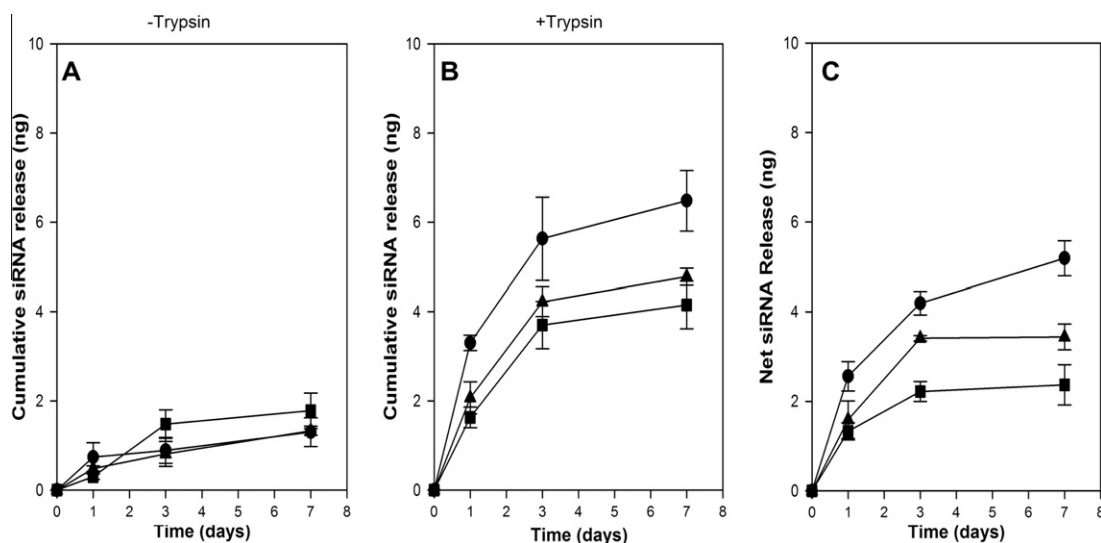


**Fig. 6.** siRNA release (in ng) from BSA NPs coated with 1 mg ml<sup>-1</sup> of 0.9 (■), 4.2 (▲) and 24 (●) kDa PLL in the presence and absence of trypsin. Trend lines are provided as a guide to the eye only. Data points represent an average of  $n \geq 3$ ; error bars are  $\pm 1$  SD. Twenty-four kilodaltons PLL-coated BSA NPs showed the highest encapsulation efficiency and a steep rise in the percent of siRNA released from the NPs in the presence of trypsin.

24 kDa PLL revealed the highest zeta-potentials. Coating of BSA NPs with low MW PLLs (0.9 and 4.2 kDa) at low concentration (0.1 mg ml<sup>-1</sup>) resulted in a dramatic increase in the particle size,

possibly because of a flocculation mechanism. The use of higher MW (24 kDa) PLL for the NP coating offered an increase in NP stability under aqueous conditions; however, it afforded the least

protection against enzymatic digestion. In fact, PLL coatings formed from shorter PLLs seemed to offer more protection against enzymatic degradation. This might be because fewer high MW molecules are required to fill the NP surface, and because high MW PLLs are prone to forming domains (i.e. loops) that are not closely associated with the NP and are easily accessible to solution enzymes. These observations will be critical when considering coating materials for developing “soft” nanoparticle-based delivery systems and especially for designing NPs with controlled sensitivity to proteolytic enzymes.

### Acknowledgements

This study was supported by Natural Sciences and Engineering Research Council of Canada (NSERC) and Chemical & Materials Engineering Department, University of Alberta, Canada.

### Appendix A. Figures with essential color discrimination

Certain figures in this article, particularly Figs. 2 and 4 are difficult to interpret in black and white. The full color images can be found in the on-line version, at doi:10.1016/j.actbio.2010.06.017.

### References

- [1] Panyam Jayanth, Labhasetwar Vinod. Biodegradable nanoparticles for drug and gene delivery to cells and tissue. *Adv Drug Deliv Rev* 2003;55:329–47.
- [2] Florence Alexander T. Issues in oral nanoparticle drug carrier uptake and targeting. *J Drug Target* 2004;12:65–70.
- [3] Gelperina Svetlana, Kisich Kevin, Iseman Michael D, Heifets Leonid. The potential advantages of nanoparticle drug delivery systems in chemotherapy of tuberculosis. *Am J Respir Crit Care Med* 2005;172:1487–90.
- [4] Nelson David L, Cox Michael M. Principles of biochemistry. 4th ed. New York: W.H. Freeman; 2004.
- [5] Yagi Nobuhiro et al. A nanoparticle system specifically designed to deliver short interfering RNA inhibits tumor growth in vivo. *Cancer Res* 2009;69:6531–8.
- [6] Rahimnejad M, Jahanshahi M, Najafpour GD. Production of biological nanoparticles from bovine serum albumin for drug delivery. *Afr J Biotechnol* 2006;5:1918–23.
- [7] Menger Fredric M, Sykes Bridget M. Anatomy of a coacervate. *Langmuir* 1998;14:4131–7.
- [8] Wang Guilin et al. Preparation of BMP-2 containing bovine serum albumin (BSA) nanoparticles stabilized by polymer coating. *Pharm Res* 2008;25:2896–909.
- [9] Merodio Marta, Arnedo Amaia, Jesús Renedo M, Irache Jaun M. Ganciclovir-loaded albumin nanoparticles: characterization and in-vitro release properties. *Eur J Pharm Sci* 2001;12:251–9.
- [10] Ko Sanghoon, Gunasekaran Sundaram. Preparation of sub-100 nm  $\beta$ -lactoglobulin (BLG) nanoparticles. *J Microencapsul* 2006;23:887–98.
- [11] Ezpeleta I, Irache JM, Gueguen J, Orecchioni AM. Properties of glutaraldehyde cross-linked vicilin nano- and microparticles. *J Microencapsul* 1997;14:557–65.
- [12] Yang Lei, Cui Fude, Cun Dongmei, Tao Anjin, Shi Kai, Lin Wenhui. Preparation, characterization and biodistribution of the lactone form of 10-hydroxycamptothecin (HCPT)-loaded bovine serum albumin (BSA) nanoparticles. *Int J Pharm* 2007;340:163–72.
- [13] Langer K, Balthasar S, Vogel V, Dinauer N, Von Briesen H, Schubert D. Optimization of the preparation process for human serum albumin (HSA) nanoparticles. *Int J Pharm* 2003;257:169–80.
- [14] Zhang Sufeng, Wang Guilin, Lin Xiaoyue, Chatzinikolaidou Maria, Jennssen Herbert P, Laub Marcus, et al. Polyethylenimine-coated albumin nanoparticles for BMP-2 delivery. *Biotechnol Prog* 2008;24:945–56.
- [15] Holmberg Krister. Handbook of applied surface and colloid chemistry. first ed. Chichester: John Wiley & Sons Ltd.; 2002.
- [16] Avgoustakis Konstantinos. Pegylated poly (lactic) and poly (lactic-co-glycolide) nanoparticles: preparation, properties and possible applications in drug delivery. *Curr Drug Deliv* 2004;1:321–33.
- [17] Li Weijun, Szoka Jr Francis C. Lipid-based nanoparticles for nucleic acid delivery. *Pharm Res* 2007;24:438–49.
- [18] Sioud M. On the delivery of small interfering RNAs into mammalian cells. *Expert Opin Drug Deliv* 2005;12:639–51.
- [19] Blackburn WH, Dickerson EB, McDonald JF, Lyon LA. Peptide functionalized nanogels for targeted siRNA delivery. *Bioconjug Chem* 2009;20:960–8.
- [20] Patil Y, Panyam J. Polymeric nanoparticles for siRNA delivery and gene silencing. *Int J Pharm* 2009;362:195–203.
- [21] Lin Wu, Garnett Martin C, Davis Stanley S, Schacht Etienne, Ferruti Paulo, Illum Lisbeth. Preparation and characterization of rose Bengal-loaded surface modified albumin nanoparticles. *J Control Release* 2001;71:117–26.